JOURNAL OF SOLID STATE CHEMISTRY 107, 428–443 (1993)

A Powder Neutron Diffraction Investigation of Structure and Cation Ordering in $Ba_{2+x}Bi_{2-x}O_{6-y}$

KENNETH P. REIS AND ALLAN J. JACOBSON*

Department of Chemistry and Texas Center for Superconductivity, University of Houston, Houston, Texas 77204

AND JACQUELINE M. NICOL

Reactor Radiation Division, National Institute of Standards and Technology, Gaithersburg, Maryland 20899

Received February 5, 1993; accepted April 7, 1993

The structures and cation ordering of several barium bismuth oxide phases, $Ba_{2+x}Bi_{2-x}O_{6-y}$ (x = 0.22, 0.28, 0.40, 0.67), have been determined at ambient temperature from constant wavelength and time-of-flight neutron powder diffraction data. The end member of the series, $Ba_2Bi(III)Bi(V)O_6$, has a monoclinic distortion of the simple cubic perovskite structure with an ordered arrangement of the Bi^{3+} and Bi^{5+} cations on the B sites. When additional barium atoms are introduced into the structure, substitution of Ba for Bi(III) occurs to give phases with the composition $Ba_2[(Bi_{1-x}Ba_x)Bi]O_6$ when $x < 0.6$. The monoclinic structure at $x = 0$ changes first to a rhombohedral structure and then to cubic as x is increased. At $x = 0.67$, the structure remains cubic but the cation distribution changes to give an unusual arrangement, represented by $Ba_{5/3}Bi_{1/3}[BaBi(V)]O_{5.67}$, with Bi^{3+} cations on the perovskite A sites and complete Ba^{2+}/Bi^{5+} ordering on the B sites.

Introduction

Substituted barium bismuth oxide phases are of considerable interest as examples of isotropic oxide structures which show superconductivity. The perovskite system $BaPb_{1-x}Bi_xO_3$ was the first example of a nontransition metal oxide phase to exhibit high temperature superconductivity with a T_c of 13 K at $x = 0.3$ (*4*) and can be thought of as the forerunner to the high-T_c copper-containing perovskite oxides subsequently discovered (*5*, *6*). In mixed oxides containing bismuth, superconductivity at 30 K was observed recently in potassium-doped $BaBiO_3$ (*7*, *8*). The $Ba_{1-x}K_xBiO_3$ phase is semiconducting until a critical doping level (x) when it becomes metallic and superconducting with a maximum T_c = 30 K at x = 0.37 (*9*). A clear correlation between structural properties and superconductivity in this phase has been examined in detail by neutron diffraction (*10*, *11*). Superconductivity has also been observed in $BaBiO_3$ doped with rubidium, 29 K (*12*); in $BaPb_{0.75}Sb_{0.25}O_3$, 3.5 K (*13*); and in $BaBi_{0.25}Tl_{0.25}Pb_{0.5}O_3$, 8 K (*14*).

All of the known superconducting phases are derived from the doubled cubic structure of $BaBiO_3$ which has a 1 : 1 ordered arrangement of Bi^{3+} and Bi^{5+} ions on the B sites (*1–3*). In contrast to the isotropic barium bismuth oxides, the cuprate superconductors have strongly anisotropic structures and properties. Consequently, synthesis of analogous layered bismuth phases is of considerable interest for further investigation of the influence of dimensionality in models

*To whom correspondence should be addressed.

0022-4596/93 $5.00

for high-temperature superconductivity. The logical candidate structures for study are the Ruddlesden–Popper (RP) phases with the general composition $Ba_{n+1}B_nO_{3n+1}$ (*16, 17*). Several members of this series are known where B = Pb, viz. $Ba_{n+1}Pb_nO_{3n+1}$ (n = 1, 3, ∞) (*18–21*). Substitution of lead by bismuth up to levels of 30% has been reported for the compounds with n = 1 and 3, and up to 50% in the n = 2 phase, but superconductivity has not been observed (*19, 21, 22*). The sole example of an RP phase with the B sites occupied only by Bi cations is the n = 2 phase $Ba_{1.7}K_{1.3}Bi_2O_7$ prepared by electrochemical synthesis in molten KOH (*23*). This composition does not show superconductivity though a theoretical study suggested that the level of potassium doping may not be optimum (*24*). Other compositions have not yet been synthesized and may be difficult to access.

Attempts to synthesize "Ba_2BiO_4" with the La_2CuO_4 structure type have so far been unsuccessful. The compound formed by heating the stoichiometry represented by "Ba_2BiO_4" in oxygen or air has a structure related to that of the doubled cubic, 1 : 1-ordered perovskite structure, $A_2[BB']O_6$. A series of $Ba_{2+x}Bi_{2-x}O_{6-y}$ phases with perovskite-related structures have been investigated by two groups (*25–27*). Itoh *et al.* reported the synthesis of single phase materials for $0 \leq x \leq 1.0$, by reaction of $BaCO_3$ and Bi_2O_3 at temperatures up to 1000°C in oxygen (*25, 27*). For the compositions $0 \leq x \leq 0.67$, oxygen contents close to stoichiometric were reported, ($0 \leq y \leq 0.1$). The small deviations from stoichiometry increased with increasing x. In this composition range, the monoclinic structure of $BaBiO_3$ changes to rhombohedral and then to cubic as x increases. Compounds with $0.8 \leq x \leq 1.0$ were synthesized similarly, but were found to be more oxygen deficient ($0.24 \leq y \leq 0.494$). Licheron *et al.* reported results for two samples prepared in air at 950°C with x = 0.5 and 0.67 (*26*). The structure of the x = 0.67 phase was determined from X-ray powder data by refinement of the integrated intensities. A cubic structure, space group $FM\bar{3}m$, with the cation distribution $Ba_2[Ba_{2/3}Bi_{1/3}]BiO_{5.67}$ was proposed. The oxygen stoichiometry was not measured directly but was calculated by assuming that all of the bismuth cations on the barium sites are Bi^{3+}.

The $Ba_{2+x}Bi_{2-x}O_{6-y}$ phases are of interest from a structural standpoint both because Ba^{2+} cations occupy the perovskite B sites and also because of the variety of possible distributions of bismuth cations in different oxidation states between the A and B cation positions. In order to investigate the structures and cation distributions in more detail, four compounds in the series with x = 0.22, 0.28, 0.40, and 0.67 have been investigated by neutron powder diffraction. Other compositions with $x \leq 0.67$ have been prepared and studied by X-ray powder diffraction.

Experimental

For the present experiments, a series of $Ba_{2+x}Bi_{2-x}O_{6-y}$ compositions ($0.05 \leq x \leq 0.67$) was prepared in air using conventional high-temperature ceramic methods. Stoichiometric mixtures of Bi_2O_3 and $BaCO_3$ were heated in alumina crucibles at 700°C (1*d*), 800°C (1*d*), 875°C (1*d*), and 900–950°C (2–5*d*). It was necessary to ensure complete reaction of $BaCO_3$ before heating at temperatures greater than 850°C, otherwise partial melting of the reaction mixture occurs. An apparent solubility limit for barium at x = 0.67 was observed using this procedure. Attempts to synthesize compounds with higher barium content always led to decomposition. For the neutron diffraction experiments, larger samples (10 g) were prepared with compositions corresponding to x = 0.22, 0.28, 0.40, and 0.67.

The oxygen contents of the samples were determined by thermogravimetric reduction in a 5% H_2/N_2 mixture. The samples were

reduced in a Dupont 990 TGA[1] system under the following conditions. The samples were heated to 600°C at a rate of 10°/min under a constant gas flow (50 ml/min) and then held at constant temperature until complete reduction to BaO and Bi metal had taken place. The differences between the final and initial weights were used to determine the oxygen contents. X-ray power diffraction measurements were made at ambient temperature using a Scintag XDS 2000 automated powder diffractometer with Cu $K\alpha$ radiation and a solid-state detector. Data were collected in 0.02° steps with a count time of 5 sec per step over the angular range $15° \leq 2\theta \leq 100°$.

For the compound with $x = 0.67$, the neutron diffraction measurements were made at ambient temperature with the high-resolution five-counter diffractometer at the National Institute of Standards and Technology. The sample (ca. 13 g) was contained in a 10-mm diameter cylindrical vanadium can and data were collected over the angular range $10° \leq 2\theta \leq 120°$ at intervals of 0.05° using a wavelength of 1.5453 Å. Data for the other samples ($x = 0.22$, 0.28, and 0.40) were collected on the neutron powder diffractometer at LANSCE, Los Alamos National Laboratory. Samples (ca. 10 g) were contained in cylindrical vanadium cans. Time-of-flight data were collected at ambient temperature using four banks of detectors located at ±148° and ±90° to the incident neutron beam. After initial inspection, the data from the +90° detector bank were excluded from the refinement due to detector problems.

Both the constant wavelength and time-of-flight powder diffraction data were analyzed by Rietveld profile analysis using the GSAS programs (*28*). Atomic, positional, thermal parameters, background, and profile coefficients were refined simultaneously. Neutron scattering lengths b_i ($\times 10^{-12}$ cm) were taken as $b_{Ba} = 0.525$, $b_{Bi} = 0.835$, and $b_O = 0.5805$. The constant wavelength data were fitted using a Gaussian peak shape modified for peak asymmetry. The full width at half maximum of the peak (w) as a function of 2θ varies according to $w = U\tan^2\theta + V\tan\theta + W$. The time-of-flight profile function used was a convolution of two back-to-back exponentials with a Gaussian. The Rietveld refinement was performed on all data points with d spacings between 0.5 and 3.0 $Å^{-1}$ (10–50 msecs time of flight). Five profile parameters and four background coefficients were used to fit the profile data for each of the three detector banks.

[1] Manufacturers are identified to provide a complete description of the experimental conditions. No endorsement by the National Institute of Standards and Technology is intended.

TABLE I

OXYGEN CONTENTS (y) AND CELL PARAMETERS OF $Ba_{2+x}Bi_{2-x}O_{6-y}$ PHASES

x	6-y	a (Å)[a]
0.0[b]	6.0[d]	4.3448(3)
0.10	6.05	4.357(3)
0.15	6.04	4.354(3)
0.22[c]	6.02	4.3619(4)
0.28[c]	6.01	4.3685(4)
0.35	5.94	4.3732(4)
0.40[c]	5.97	4.3750(3)
0.45	5.93	4.3736(3)
0.50	5.94	4.3760(3)
0.55	5.92	4.3777(4)
0.60	5.94	4.3807(5)
0.67[c]	5.67	4.3997(3)

[a] Pseudocubic cell parameter.
[b] Average value of data from References 1–4.
[c] Data from neutron diffraction measurements.
[d] Values of y are ±0.03.

Results

Synthesis and Characterization

The compositions $Ba_{2+x}Bi_{2-x}O_{6-y}$, $O \leq x \leq 0.67$, all have structures related to a 1 : 1-ordered cubic perovskite ($A_2BB'O_6$) with barium atoms on the perovskite B sites, as reported previously. The K_2NiF_4 structure type, "Ba_2BiO_4," does not form at any

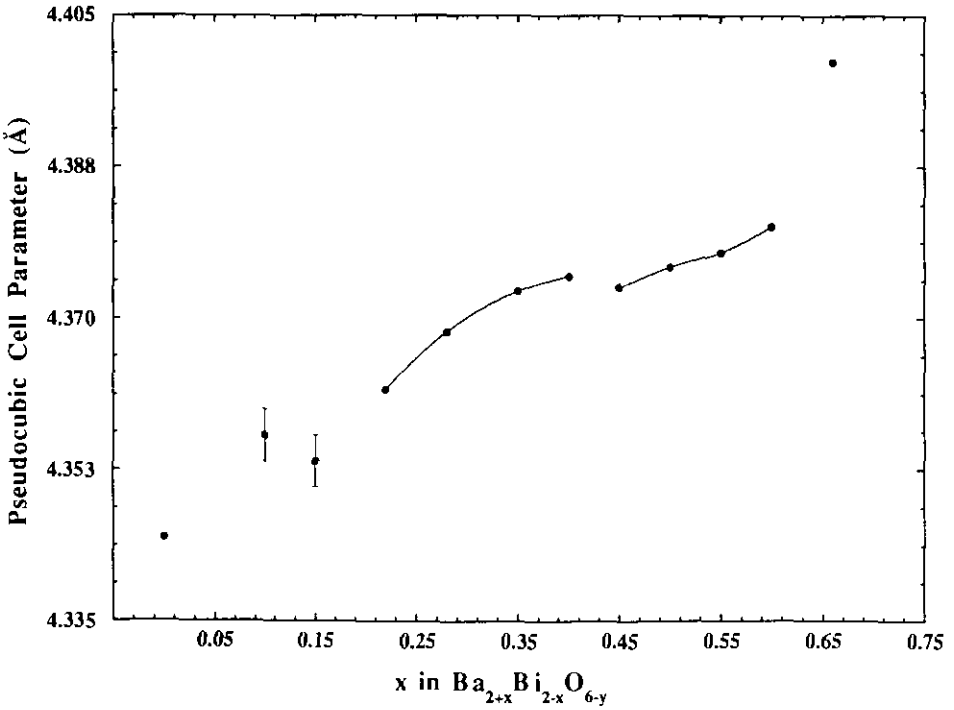

FIG. 1. Pseudocubic perovskite a parameter versus composition for $Ba_{2+x}Bi_{2-x}O_{6-y}$.

value of x under the synthesis conditions used here. The pseudo-cubic perovskite a parameters (calculated as the cube root of the cell volume) for the phases prepared in this work are given in Table I and are shown as a function of composition in Fig. 1. The values determined for the compositions $x = 0.10$ and 0.15 are less precise than the other data because of difficulty in determining the true cell symmetry from the X-ray data. The peaks are insufficiently well resolved to distinguish between monoclinic and rhombohedral unit cells. The oxygen contents of the samples determined from hydrogen reduction are also given in Table I. For $x \leq 0.60$, the oxygen contents are close to stoichiometric within the error of the determination (± 0.03), but at $x = 0.67$ the sample is significantly oxygen deficient ($y = 0.33$; see below).

Replacement of Bi^{3+} ($r = 1.03$ Å) or Bi^{5+} ($r = 0.76$ Å) cations on the octahedral sites by the larger barium cation ($r = 1.35$ Å) causes an increase in the unit cell constant with increasing barium content, though the variation is not linear. Discontinuous changes in a are observed between $x = 0.15$ and 0.22, $x = 0.40$ and 0.45, $x = 0.60$ and 0.67. At $x = 0$, the unit cell is monoclinic but the neutron diffraction data (below) clearly show that at $x = 0.22$ the symmetry is rhombohedral. The discontinuity at low x may be a consequence of this change in symmetry. However, the X-ray data for the intermediate compounds ($x = 0.1$, 0.15) cannot clearly distinguish between rhombohedral or monoclinic structures. A discontinuity between $x = 0.1$ and 0.2 is also apparent in the previous data (*25*, *27*) but was not discussed. The discontinuity between $x = 0.40$ and 0.45 coincides with the apparent change from rhombohedral to cubic symmetry. Overall, the lattice parameters reported here agree within ± 0.002 Å with the values reported by Itoh *et al.* for the compositions $0.2 \leq x \leq 0.6$ (*25*, *27*). The cell constant reported for the $x = 0.5$ phase by the French group (*26*) is significantly smaller than the

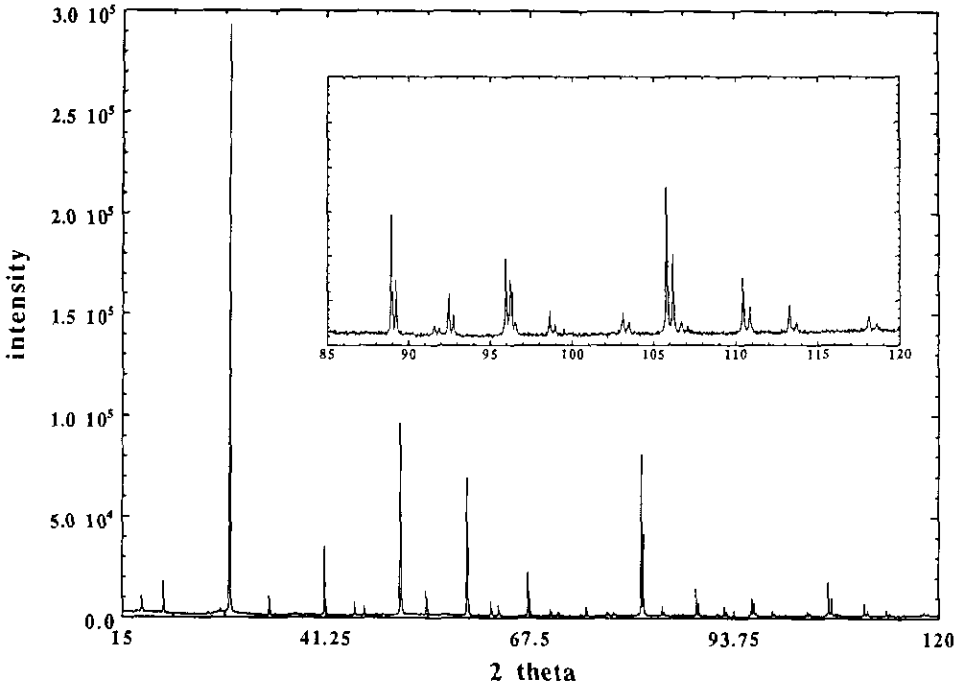

FIG. 2. X-ray powder diffraction data for $Ba_{2.67}Bi_{1.33}O_{5.67}$ with Cu $K\alpha$ radiation. The $K\alpha_1$ and $K\alpha_2$ lines are resolved but no distortion is observed.

other values. If the series is written as $Ba_2[Ba_xBi(III)_{1-x}]Bi(V)O_{6-y}$, with barium progressively replacing Bi(III) on the *B* site, then $y = x/2$. However, the Bi(III) cations are almost completely oxidized to Bi(V) since the oxygen content is observed to be close to stoichiometric when $x \leq 0.60$. A highly disordered cation distribution must result, with Ba^{2+}, Bi^{3+}, and Bi^{5+} cations all residing on the same site.

The $x = 0.67$ phase differs from the rest of the series in two respects. The stoichiometry indicates the presence of a significant number of oxygen vacancies ($y = 0.33$) and the cubic lattice parameter is larger than expected by extrapolation of the data for the other compounds in the series. No evidence is observed in the X-ray data for any distortion from cubic symmetry (Fig. 2). The oxygen stoichiometry corresponds to one-quarter of the bismuth cations being in the Bi(III) oxidation state and is reproducible in several samples prepared by the same procedure. Attempts to increase the oxygen content by heating the $x = 0.67$ composition in oxygen at high temperatures, followed by annealing at lower temperature (400°C) in oxygen, did not increase the oxygen content of the samples. Oxygen nonstoichiometry corresponding to $y = 0.33$, at $x = 0.67$, was assumed but not directly measured in the study by Licheron *et al.* (*26*). In contrast, Itoh *et al.* reported an oxygen content close to stoichiometric ($y = 0.05$) for the $x = 0.67$ phase. The marked difference in oxygen stoichiometry for our $x = 0.67$ composition suggests that the cation distribution is different compared with the arrangement in the lower barium content phases.

In general, the X-ray diffraction patterns for the different compositions are similar except for changes due to the increase in cubic lattice parameter with increasing x. All patterns show the superlattice lines with $h, k, l = 2n + 1$ resulting from ordering of the *B* cations. Figure 3 illustrates how the

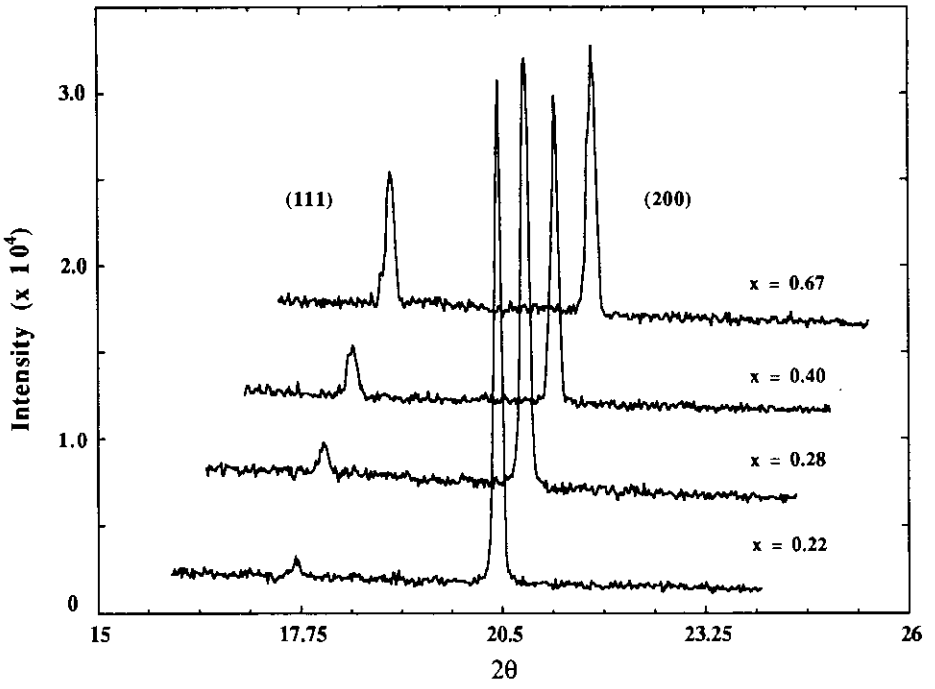

FIG. 3. X-ray diffraction data for $Ba_{2+x}Bi_{2-x}O_{6-y}$ phases showing the relative increase with increasing x in the intensity of the cubic (111) reflection compared with the (200).

X-ray intensities of the cubic (111) and (200) reflections evolve with increasing barium content. At the $x = 0.67$ composition, the superlattice lines are significantly stronger than for the other compositions. Qualitative intensity calculations (using the Lazy Pulverix program) indicated that the superlattice lines increase in intensity when Ba^{2+} ions are substituted for Bi^{3+} ions on the B site. At $x = 0.67$, however, the intensities of the superlattice lines agree much better with the results calculated for a model corresponding to complete substitution of the Bi (III) site by Ba ions giving a cation distribution $[Ba_{5/3}Bi_{1/3}][BaBi(V)]O_{5.67}$. A transfer of Bi cations from the B sites to the A sites increases the scattering difference between the B and B' sites, thereby producing an enhancement of the intensities of the superlattice peaks. The Bi(III) cations located on the perovskite A sites are expected to be nonoxidizable and can thus account for the oxygen nonstoichiometry. A quantitative neutron diffraction verification of this structural model for the $x = 0.67$ phase is described in the next section.

Neutron Diffraction

$Ba_2[Ba_xBi_{1-x}]BiO_6$, $x = 0.22, 0.28, 0.40$. The parent of the present series of compounds, $BaBiO_3$, has a monoclinic distortion of the simple cubic perovskite lattice. The distortion arises both from tilts of BO_6 octahedra as described by Glazer (*28, 29*) and ordering of bismuth cations with two different oxidation states as indicated by $Ba_2Bi(III)Bi(V)O_6$. The distortion results in a larger unit cell with cell constants $a\sqrt{2} \times a\sqrt{2} \times 2a$, $\beta \neq 90°$, and space group $I2/m$ (No. 12).

The neutron diffraction data for the phase $Ba_2[Ba_{0.22}Bi_{0.78}]BiO_6$ clearly indicated a distortion from cubic symmetry as expected from the X-ray data. The distortion can be

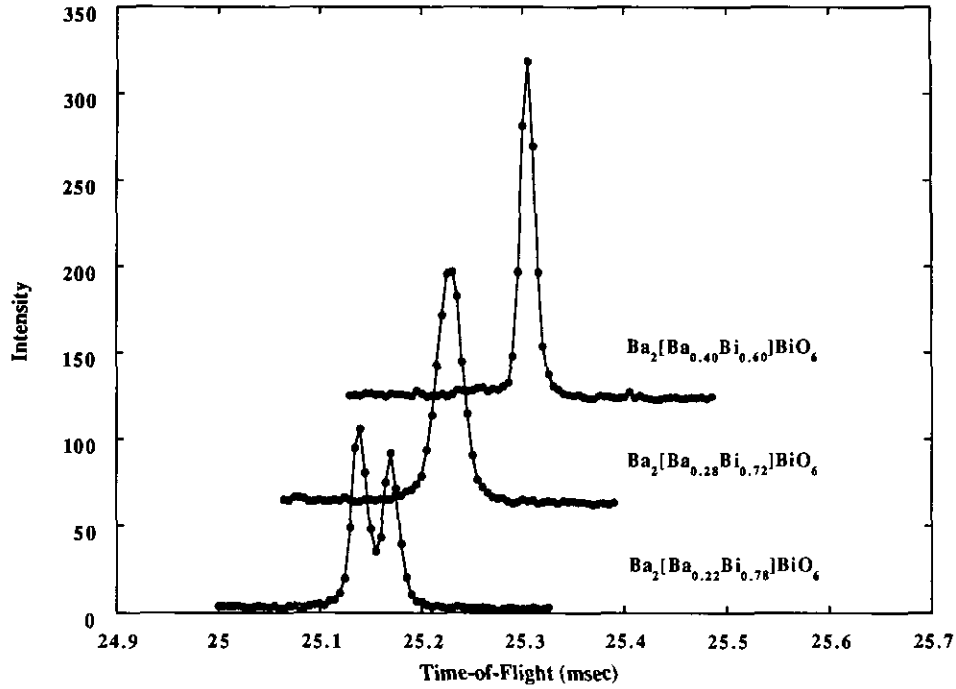

FIG. 4. Neutron diffraction data for $Ba_{2+x}Bi_{2-x}O_{6-y}$ at $x = 0.22, 0.28, 0.40$. The data are for the (440) reflection of the doubled cubic unit cell. The (440) reflection splits into (422) and (202) (with $d = 1.5393$ and 1.5450 Å, respectively) in the primitive rhombohedral cell at $x = 0.22$ and is broadened at $x = 0.28$.

seen easily in the neutron time-of-flight data in the range. 1.5 Å $\leq d \leq$ 2.0 Å (Fig. 4). By analogy with the structure of $BaBiO_3$, an initial refinement of the structure was attempted in the monoclinic space group $I2/m$ which corresponds to B cation order and two negative octahedral tilts ($a^0b^-b^-$ in Glazer's notation). An alternative monoclinic structure with one additional tilt ($a^-b^-b^-$, space group $P2_1/n$ (No. 15)), that has been observed previously in several 1 : 1-ordered perovskite structures, was also tested (*30, 31*). The splittings of the peaks could not be reproduced with either model and a satisfactory refinement of the intensity data could not be obtained. Further inspection of specific peaks indicated that the unit cell was rhombohedral. The data were consequently refined in space group $R\bar{3}$ (No. 60) corresponding to the tilt system $a^-a^-a^-$ ($R\bar{3}c$) with ordered cations. The additional barium atoms in the structure are located on the Bi(III) cation site. The thermal parameters for the Ba and Bi(III) atoms were constrained to be equal and the total site occupancy was constrained to unity for this refinement and also for the refinements of the data at the other compositions. The simultaneous occupancy of the Bi(III) site by both barium and bismuth cations introduces considerable disorder into the structure which cannot easily be modeled. The presence of both (III) and (V) oxidation states of the bismuth atoms on this site adds to the difficulty of finding an adequate representation of the structure. At best, only an average structure can be determined and large thermal parameters are expected. Refinements for the $x = 0.22$ composition, in which isotropic thermal parameters and the site occupancy of the Bi(III) position were varied, resulted in poor fits to the data. Such

TABLE II

REFINED PROFILE AND STRUCTURAL PARAMETERS FOR $Ba_2[Ba_{0.22}Bi_{0.78}]BiO_6$

Atom	Site	x	y	z	*Occ.*	u_{iso}(Å^2)
Ba1	2*c*	0.2481(4)	x	x	1.0	0.017(1)
Ba2	1*b*	0.5	0.5	0.5	0.18(3)	0.014(1)
Bi1	1*a*	0	0	0	1.0	0.005(1)
Bi2	1*b*	0.5	0.5	0.5	0.82(3)	0.014(1)
O1	6*f*	−0.2431(1)	0.1969(4)	0.2850(4)	1.0	—
u_{aniso}(Å^2): 0.043(1)						
		0.029(1)				
			0.022(1)	−0.011(2)	−0.001(1)	−0.016(1)

R_{wp} = 9.8% R_p = 6.6%

Cell constants: a = 6.1573(4)Å, α = 60.247(1), $R\bar{3}$

Bond lengths(Å)

Ba1–O1	3.101(7)	Ba1–O1	3.364(1)
Ba1–O1	3.081(7)	Ba2/Bi2–O1	2.276(3)
Ba1–O1	2.819(1)	Bi1–O1	2.120(3)

refinements gave large thermal parameters and unreasonable values for the bond distances and composition. A significantly improved refinement was obtained when the static disorder was represented by anisotropic oxygen thermal parameters. The results from the refinement with this model for the x = 0.22 composition are shown in Table II and in Fig. 5. The refined site occupancy for the Bi(III) site with this model is in agreement with the known composition and the bond distances are more reasonable. The refinement is only moderately sensitive to the precise value of the composition, in part due to the absence of the cubic (111) reflection from the range of time-of-flight data which could be collected. The static disorder inherent in this phase is apparent in the large values of the thermal parameters of all atom positions in the final model. The agreement between the observed and calculated profiles indicates, however, that little further information can be extracted from the powder data.

Both the X-ray and neutron data for $Ba_2[Ba_{0.28}Bi_{0.78}]BiO_6$ appear to indicate a face-centered doubled-cubic unit cell. More detailed inspection of the neutron data indicated that several peaks expected to be split in rhombohedral symmetry were significantly broadened (see, e.g., Fig. 4). The structure was refined, therefore, with the same model that was used for the sample with x = 0.22. The results are shown in Table III. The overall fit to the data with the rhombohedral model is significantly better than could be obtained with a cubic $Fm\bar{3}m$ model which was tested for comparison. The rhombohedral angle, 60.136°, is smaller than the value observed at x = 0.22 (α = 60.247°). The static disorder is again reflected in the large thermal parameters.

No departure from cubic symmetry could be detected in the data for the phase $Ba_2[Ba_{0.40}Bi_{0.60}]BiO_6$. The structure was refined in space group $Fm\bar{3}m$ (No. 225) with anisotropic oxygen thermal parameters. The anisotropic refinement showed that the apparent thermal motion is very large (u = 0.09 Å^2) in directions perpendicular to the Ba/Bi–O–Bi axis. Better refinements were obtained when the disorder was represented by placing the oxygen atoms either on (0, y, z) or (x, x, z) sites with $\frac{1}{4}$ occupancies. Refinement of oxygen on either position substantially reduced all thermal parameters. Result for the (0, y, z) refinement are given in Table IV. The occupancies for the

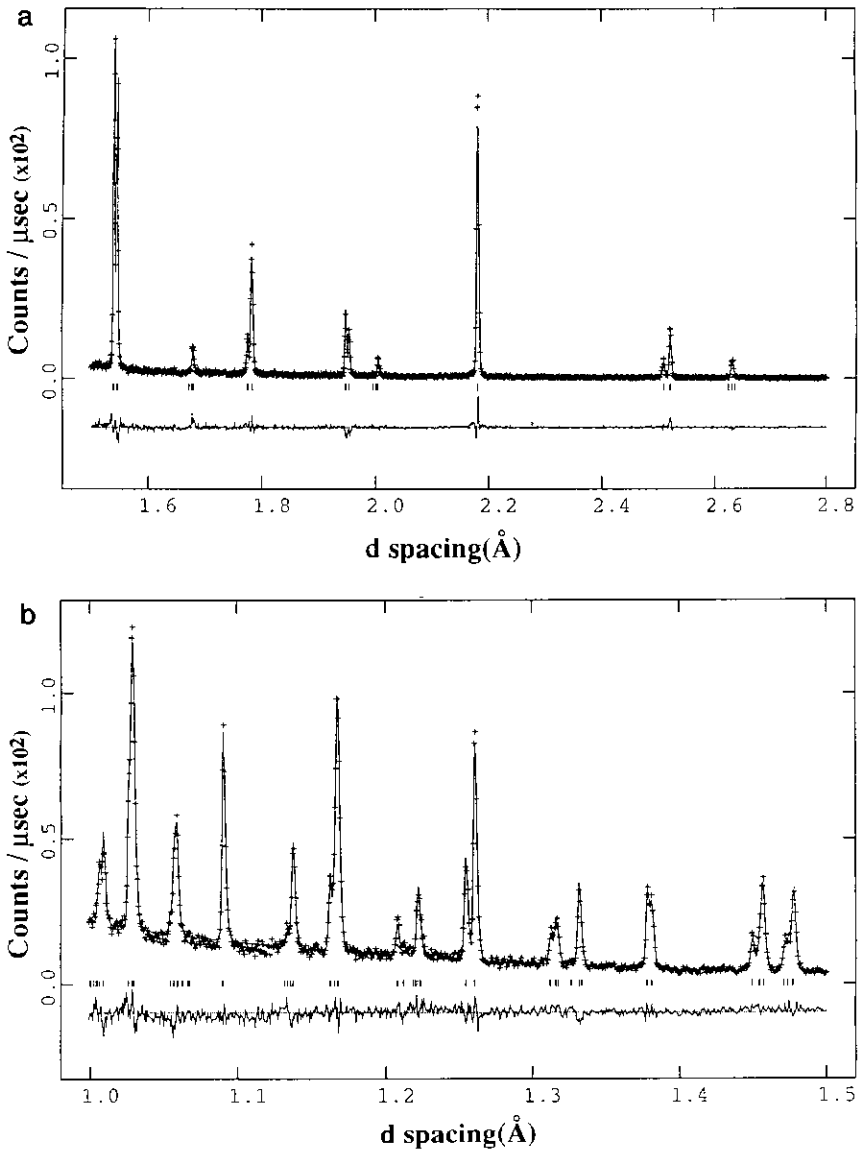

FIG. 5. Time-of-flight neutron diffraction data for $Ba_2[Ba_{0.72}Bi_{0.79}]BiO_6$. The + symbols are the experimental points and the line is the fit to the data. The bottom curve is the difference and the small vertical lines are the positions of the contributing Bragg reflections.

Bi(III) site are in agreement with the expected composition.

$Ba_{2.67}Bi_{1.33}O_{5.83}$. No evidence was observed in either X-ray or neutron data at the $x = 0.67$ composition for any departure from cubic symmetry and all reflections indicated face centering. The face-centered-cubic unit cell was confirmed also in a high-resolution synchrotron powder diffraction experiment at NSLS Brookhaven. Consequently, the structure was refined from the neutron data in space group $Fm\bar{3}m$. Initial refinements with all of the bismuth atoms confined to the *B* sites were unsatisfactory. A mixed Ba/Bi *B* site model always gave a noticeable discrepancy with respect to the

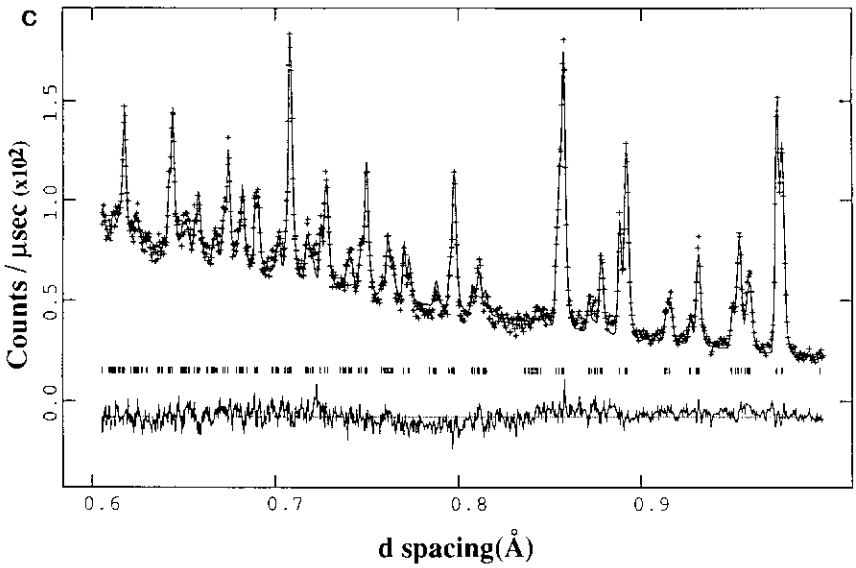

FIG. 5—*Continued*

(111) and (311) superlattice reflections with calculated peak intensities lower than the observed values (the (111) reflection which was outside of the time-of-flight range is present in the NIST constant wavelength data). As can be seen in Fig. 3, the (111) superlattice line corresponding to the ordering of B cations is significantly larger at $x = 0.67$ than for the other compositions. The difference cannot only arise from increasing Ba content. As described above, qualitative X-ray intensity calculations indicate that the two distinct *B* sites are completely occupied by Ba^{2+} and by Bi^{5+} ions

TABLE III

REFINED PROFILE AND STRUCTURAL PARAMETERS FOR $Ba_2[Ba_{0.28}Bi_{0.72}]BiO_6$

Atom	Site	*x*	*y*	*z*	*Occ.*[a]	u_{iso}(Å²)
Ba1	2*c*	0.2456(5)	*x*	*x*	1.0	0.020(1)
Ba2	1*b*	0.5	0.5	0.5	0.28	0.016(1)
Bi1	1*a*	0	0	0	1.0	0.006(1)
Bi2	1*b*	0.5	0.5	0.5	0.72	0.016(1)
O1	6*f*	−0.2435(15)	0.2030(5)	0.2781(5)	1.0	—

u_{aniso}(Å²): 0.048(2) 0.033(1) 0.031(2) −0.010(3) 0.003(3) −0.022(1)

Cell constants: $a = 6.1717(4)$Å, $\alpha = 60.136(1)$, $R\bar{3}$

Bond lengths(Å)

Ba1–O1	3.130(1)	Ba1–O1	3.328(2)
Ba1–O1	3.059(1)	Ba2/Bi2–O1	2.279(4)
Ba1–O1	2.863(2)	Bi1–O1	2.114(4)

[a] Site occupancies not refined.

TABLE IV

REFINED PROFILE AND STRUCTURAL PARAMETERS FOR $Ba_2[Ba_{0.40}Bi_{0.60}]BiO_6$

Atom	Site	x	y	z	$Occ.$	u_{iso}(Å^2)
Ba1	8c	0.25	0.25	0.25	1.0	0.038(1)
Ba2	4b	0.5	0.5	0.5	0.45(4)	0.035(1)
Bi1	4a	0	0	0	1.0	0.012(1)
Bi2	4b	0.5	0.5	0.5	0.55(4)	0.035(1)
O1	96j	0	0.0347(2)	0.2392(3)	0.25	0.032(1)

R_{wp} = 11.3% R_p = 8.4%

Cell constants: a = 8.7501(1)Å, $Fm\bar{3}m$

Bond lengths(Å)

Ba1–O1	2.888(2)	Ba2/Bi2–O1	2.302(3)
Ba1–O1	3.317(2)	Bi1–O1	2.115(3)

with the excess bismuth atoms transferred to the A sites to maintain stoichiometry. Refinement of the neutron data with this model gave significantly improved results. The occupancies of the A and B sites were in good agreement with the cation distribution $Ba_{5/3}Bi_{1/3}[BaBi]O_{5.67}$. Various other starting models for the cation distribution were evaluated but all resulted in the same final cation arrangement. The refined oxygen thermal parameter is very large indicative of static disorder. Better refinements in the cubic model were again obtained when the disorder was represented by placing the oxygen atoms on (0, y, z) sites with $\frac{1}{4}$ occupancy. The final results for this model are given in Table V and Fig. 6.

Discussion

The present results confirm that the $Ba_{2+x}Bi_{2-x}O_{6-y}$ compounds all have structures related to a 1 : 1 ordered cubic perovskite. The neutron diffraction data for the compounds with x = 0.22, 0.28, and 0.40 show that the excess barium atoms are accommodated on the perovskite B sites to

TABLE V

REFINED PROFILE AND STRUCTURAL PARAMETERS FOR $Ba_{1.67}Bi_{0.33}[BaBi]O_{5.67}$

Atom	Site	x	y	z	$Occ.$[a]	u_{iso}(Å^2)
Ba1	8c	0.25	0.25	0.25	0.86	0.042(1)
Ba2	4b	0.5	0.5	0.5	1.0	0.016(1)
Bi1	8c	0.25	0.25	0.25	0.14	0.042(1)
Bi2	4a	0.0	0.0	0.0	1.0	0.001(1)
O1	96j	0.0	0.0352(6)	0.2319(4)	0.236	0.015(2)

R_{wp} = 10.7% R_p = 8.1%

Cell constants: a = 8.7997(5)Å, $Fm\bar{3}m$

Bond lengths(Å)

Bi1/Ba1–O1	2.907(4)	Ba2–O1	2.354(4)
Bi1/Ba1–O1	3.337(4)	Bi2–O1	2.088(3)

[a] Occupancies fixed in final refinement.

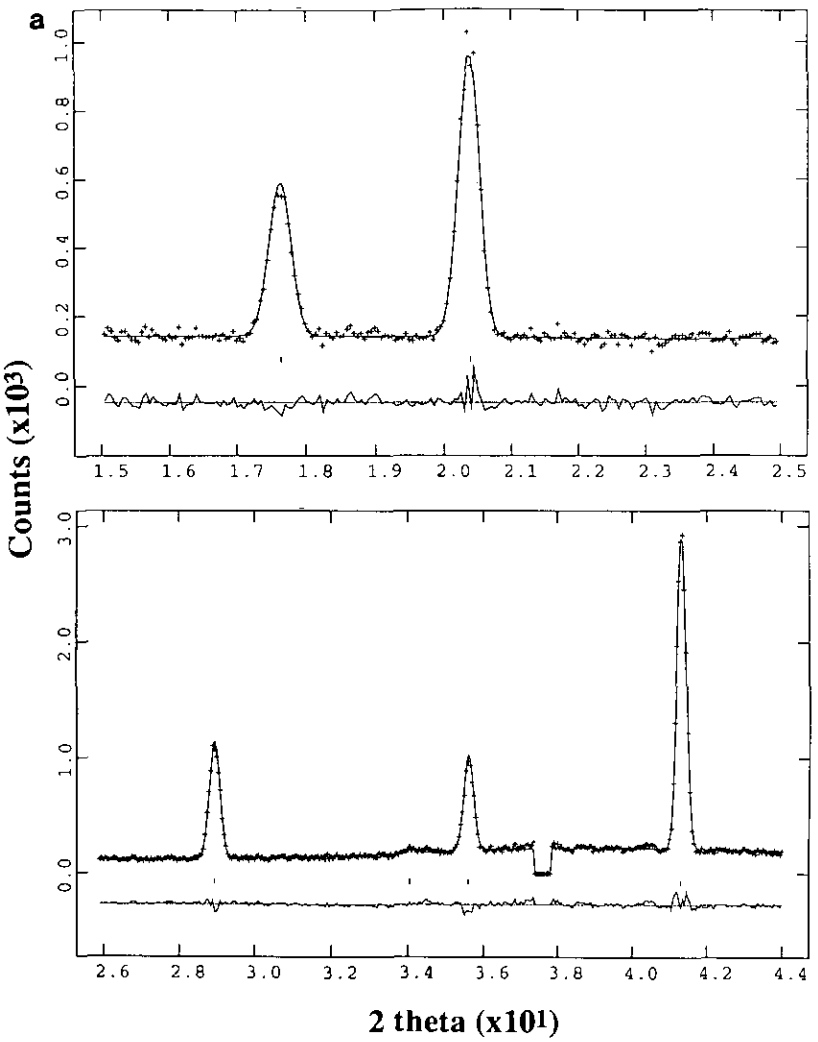

FIG. 6. Neutron diffraction data at $\lambda = 1.5$ Å for $Ba_{1.67}Bi_{0.33}[BaBi]O_{5.67}$. The lines and + symbol are as in Fig. 5. Between 37 and 38° 2θ a small impurity peak was excluded from the refinement.

give a 1 : 1 ordered distribution. One *B* site is solely occupied by Bi^{5+} ions but the other contains a mixture of barium and bismuth cations. As discussed earlier, the oxygen contents of the $x = 0.22$, 0.28, and 0.4 phases are close to stoichiometric. Consequently, in this composition range Ba^{2+}, Bi^{3+}, and Bi^{5+} cations must all occupy the same *B'* site. The composition with $x = 0.4$, for example, corresponds to the cation distribution $Ba_2[Ba_{0.22}Bi^{3+}_{0.67}Bi^{5+}_{0.11}]BiO_6$. The random distribution of cations with different sizes and charges on the *B* sites and the resulting static disorder results in the large thermal motion observed for the oxygen atoms.

The bond distances are given in Tables II–IV. In $Ba_2Bi(III)Bi(V)O_6$, the average Bi^{3+}–O and Bi^{5+}–O distances are 2.262 and 2.141 Å, respectively (*3*). As the barium content increases in the series reported here, the average Ba/Bi–O distance increases and the Bi^{5+}–O bond distance decreases slightly. The Bi(V)–O bond distances

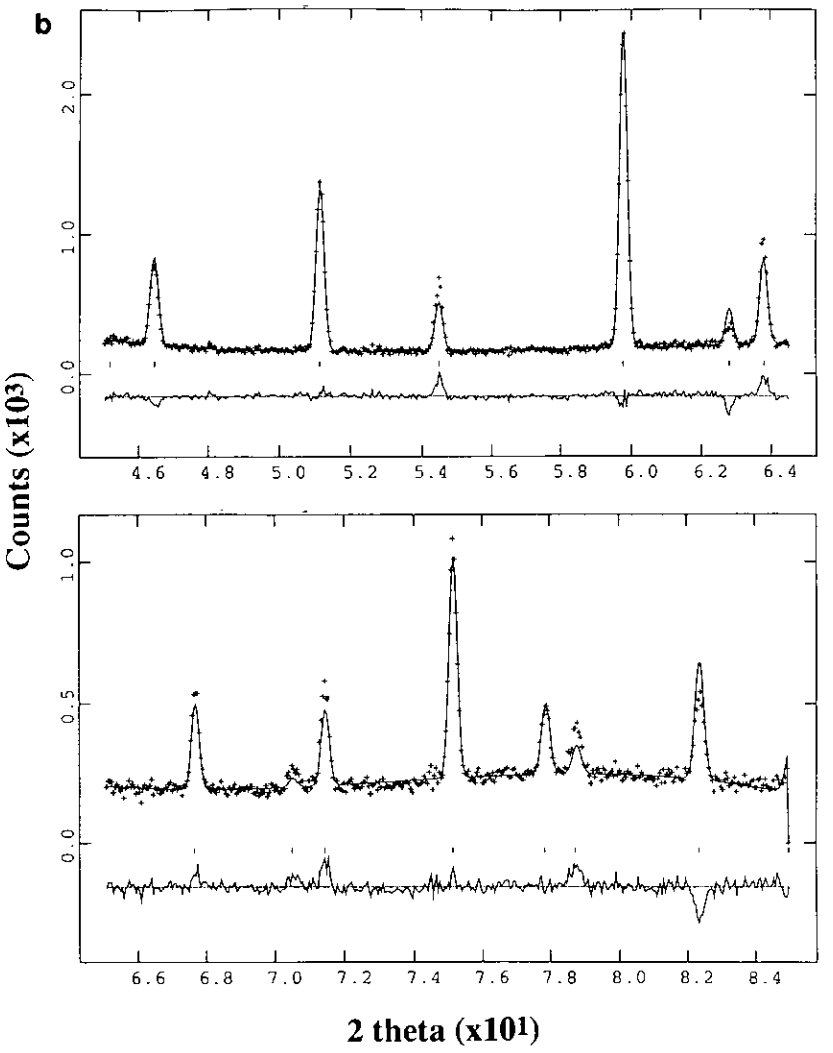

FIG. 6—*Continued*

(2.09–2.12 Å) are in the expected range but the Ba/Bi–O bond distances are about 0.2 Å shorter than predicted from the ionic radii. The precise values are, however, dependent on the model used to represent the static disorder.

The compound with $x = 0.67$ has a stoichiometric ordered arrangement of Ba^{2+} and Bi^{5+} cations on the *B* sites. In order to maintain the 2/1 ratio of barium to bismuth atoms, some Bi^{3+} cations are also located on the *A* sites and, in contrast to the lower barium content phases, the compound is oxygen nonstoichiometric. The unusual cation distribution adopted at $x = 0.67$ is energetically favored over the arrangement $Ba_2[Ba^{2+}_{0.67}Bi^{5+}_{0.33}]Bi^{5+}O_6$ that would result from an extrapolation of the cation distribution determined for the lower x phases. A distribution with Ba^{2+} and Bi^{5+} ordered on the *B* sites is favored over a structure with two cations of very different size and charge on the same site. The compound $Ba_{5/3}Bi_{1/3}[BaBi]O_{5.67}$ that results from this cation rearrangement cannot be completely stoichiometric because any additional Bi(V)

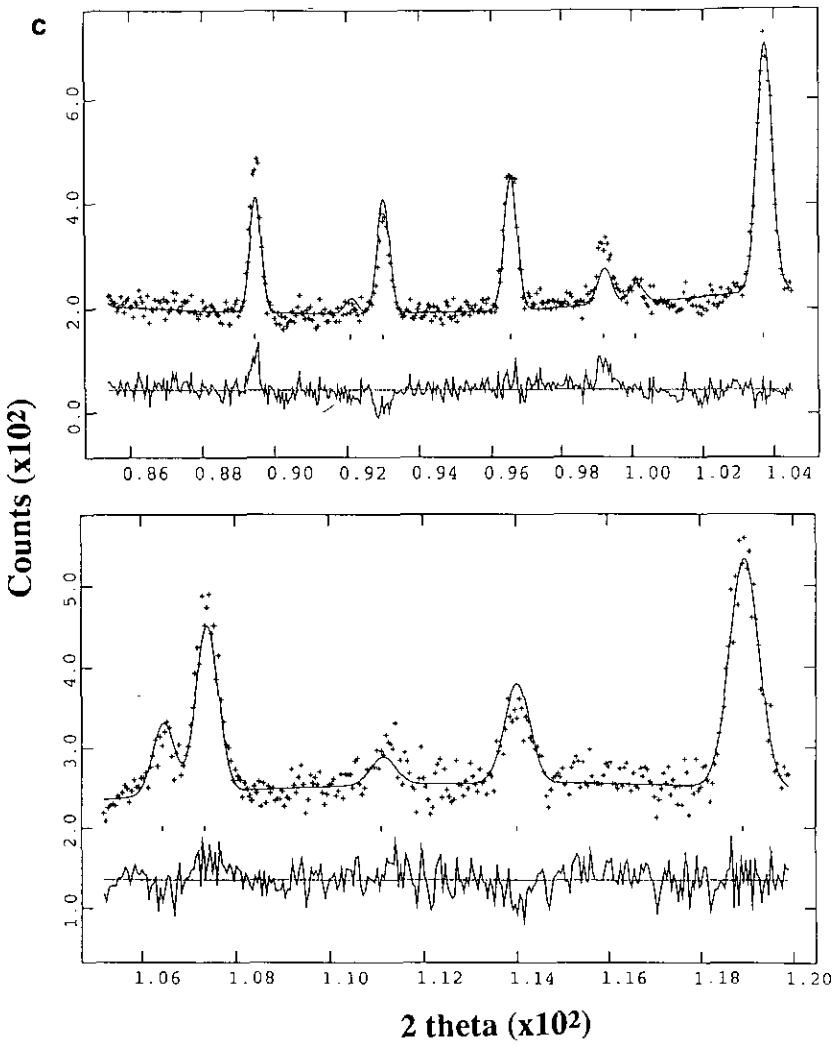

FIG. 6—*Continued*

cations generated by further oxidation would be too small for the twelve coordinate perovskite *A* sites. The $x = 0.67$ composition is rigorously cubic which is surprising because cubic symmetry imposes an average *B*–O bond distance which is too small. Normally, in perovskite structures coupled rotations of the BO_6 octahedra lead to optimum *B*–O and *A*–O bond distances. Such octahedral rotations, however, always lower the symmetry of the unit cell. In the $x = 0.67$ phase, the Ba–O distance is 2.38 Å, significantly shorter than the value of 2.79 Å expected from ionic radii but the cell remains cubic. The absence of any distortion is likely to be due to the presence of oxygen vacancies which act to uncouple the octahedral tilts and permit a disordered arrangement of oxygen positions. A related situation was recently reported for K_3C_{60} which also appears to be a face-centered cubic but is disordered (*35*).

Summary and Conclusions

The structures and cation ordering for four members of the series $Ba_{2+y}Bi_{2-y}O_{6-y}$

have been determined from powder neutron diffraction data. The compounds undergo progressive structural transformations from monoclinic to rhombohedral to cubic as x increases. Barium atoms replace Bi(III) on the B site for $x < 0.6$, but at $x = 0.67$ a unique cation distribution is observed. The perovskite B sites are occupied by Ba^{2+} and Bi^{5+} in an ordered arrangement, with some Bi(III) cations located on the A sites. The overall structure corresponds to $Ba_{5/3}Bi_{1/3}[BaBi]O_{5.67}$. Substantial cation disorder is present in all of the compositions investigated and only average structures have been determined. Significant diffuse scattering resulting from the cation disorder is observed in electron diffraction patterns and will be described in a future report. Finally, we note that cation distributions in these materials are sensitive to redox and thermal history and that other structures at the same composition can be obtained by modifications of the synthesis procedures.

Acknowledgments

The authors thank the Robert A. Welch Foundation (Grant E-1207) for support of this work. The work has benefited from the use of facilities at the Manuel Lujan, Jr., Neutron Scattering Center, a national user facility funded as such by the DOE/Office of Basic Energy Sciences. We also thank J. A. Goldstone and W. T. A. Harrison for help in collecting the neutron time-of-flight data and J. Hriljac for providing the synchrotron X-ray data.

References

1. D. E. Cox and A. W. Sleight, *Solid State Commun.* **19,** 969 (1976).
2. D. E. Cox and A. W. Sleight, in "Proc. International Conference on Neutron Scattering, Gatlinberg" (R. M. Moon, Ed.), National Technical Information Service, 1976.
3. G. Thornton and A. J. Jacobson, *Acta Crystallogr. Sect. B* **34,** 351 (1978).
4. C. Chaillout, A. Santoro, J. P. Remeika, A. S. Cooper, and G. P. Espinosa, *Solid State Commun.* **65,** 1363 (1988).
5. A. W. Sleight, J. L. Gillson, and P. E. Bierstedt, *Solid State Commun.* **17,** 27 (1975).
6. J. G. Bednorz and K. A. Muller, *Z. Phys., B* **64,** 189 (1986).
7. M. K. Wu, J. R. Ashburn, C. J. Torng, P. H. Hor, R. L. Meng, L. Gao, Z. J. Huang, Y. Q. Wang, and C. W. Chu, *Phys. Rev. Lett.* **58,** 908 (1987).
8. R. J. Cava, B. Batlogg, J. J. Krajewski, R. C. Farrow, L. W. J. Rupp, A. E. White, K. T. Short, W. F. J. Peck, and T. V. Kometani, *Nature* **332,** 814 (1988).
9. L. F. Mattheiss, E. M. Gyorgy, and D. W. J. Johnson, *Phys. Rev. B* **37,** 3745 (1988).
10. D. G. Hinks, B. Dabrowski, J. D. Jorgensen, A. W. Mitchell, D. R. Richards, S. Pei, and D. Shi, *Nature* **333,** 836 (1988).
11. S. Pei, J. D. Jorgensen, B. Dabrowski, D. G. Hinks, D. R. Richards, A. W. Mitchell, J. M. Newsam, S. K. Sinha, D. Vaknin, and A. J. Jacobson, *Phys. Rev. B* **41,** 4126 (1990).
12. S. Pei, J. D. Jorgensen, D. G. Hinks, B. Dabrowski, D. R. Richards, A. W. Mitchell, Y. Zheng, J. M. Newsam, S. K. Sinha, D. Vaknin, and A. J. Jacobson, *Physica C* **162–164,** 556 (1989).
13. I. Tomeno and K. Ando, *Phys. Rev. B: Condens. Matter* **40,** 2690 (1989).
14. R. J. Cava, B. Batlogg, G. P. Espinosa, A. P. Ramirez, J. J. Krajewski, W. F. J. Peck, L. W. J. Rupp, and A. S. Cooper, *Nature* **339,** 291 (1989).
15. S. Li, K. V. Ramanujachary, and M. Greenblatt, *Physica C (Amsterdam)* **166,** 535 (1990).
16. S. N. Ruddlesden and P. Popper, *Acta Crystallogr.* **10,** 538 (1957).
17. S. N. Ruddlesden and P. Popper, *Acta Crystallogr.* **11,** 54 (1958).
18. G. Wagner and H. Binder, *Z. Anorg. Allg. Chem.* **298,** 18 (1959).
19. W. T. Fu, H. W. Zandbergen, Q. Xu, J. M. van Ruitenbeek, L. J. De Jongh, and G. van Tendeloo, *Solid State Commun.* **70,** 1117 (1989).
20. G. Thornton and A. J. Jacobson, *Mater. Res. Bull.* **11,** 837 (1976).
21. R. J. Cava, H. Takagi, H. W. Zandbergen, B. Hessen, J. J. Krajewski, and W. F. Peck, Jr., *Phys. Rev. B* **46,** 14101 (1992).
22. Q. Xu, W. T. Fu, J. M. van Ruitenbeek, and L. J. De Jongh, *Physica C* **167,** 271 (1990).
23. R. J. Cava, T. Siegrist, W. F. Peck, Jr., J. J. Krajewski, B. Batlogg, and J. Rosamilia, *Phys. Rev. B* **44,** 9746 (1991).
24. L. F. Mattheiss, *Phys. Rev. B* **45,** 12528 (1992).
25. M. Itoh, T. Sawada, R. Liang, H. Kawaji, and T. Nakamura, *J. Solid State Chem.* **87,** 245 (1990).
26. M. Licheron, F. Gervais, J. Courtures, and J. Choisnet, *Solid State Commun.* **75,** 759 (1990).
27. M. Itoh, T. Sawada, R. Liang, H. Kawaji, and T. Nakamura, *Solid State Ionics* **49,** 57 (1991).
28. A. C. Larson and R. B. Von Dreele, General Structure Analysis System, LANSCE, MS-H805,

Los Alamos National Laboratory, Los Alamos, NM 87545.

30. R. A. Beyerlein, A. J. Jacobson, and K. R. Poeppelmeier, *J. Chem. Soc. Chem. Commun.* 225 (1988).
31. A. M. Glazer, *Acta Crystallogr. Sect. B* **28,** 3384 (1972).
32. A. M. Glazer, *Acta Crystallogr. Sect. A* **31,** 756 (1975).
33. W. A. Groen, F. P. F. van Bukel, and D. J. W. Lido, *Acta. Crystallogr. Sect. C* **42,** 1472 (1988).
34. M. P. Attfield, P. D. Battle, S. Bollen, T. C. Gibb, and R. J. Whitehead, *J. Solid State Chem.* **100,** 37 (1992).
35. P. W. Stephens, L. Mihaly, P. L. Lee, R. L. Whetten, S-M. Huang, R. Kaner, F. Diederich, and K. Holczer, *Nature* **351,** 632 (1992).